Acta Pharmacologica Sinica

ARTICLE

1-Indanone retards cyst development in ADPKD mouse model by stabilizing tubulin and down-regulating anterograde transport of cilia

Xiao-wei Li[1], Jian-hua Ran[2], Hong Zhou[1], Jin-zhao He[1], Zhi-wei Qiu[1], Shu-yuan Wang[1], Meng-na Wu[2], Shuai Zhu[1], Yong-pan An[1], Ang Ma[1], Min Li[1], Ya-zhu Quan[1], Nan-nan Li[1], Chao-qun Ren[1] and Bao-xue Yang[1,3]

Autosomal dominant polycystic kidney disease (ADPKD) is the most common inherited kidney disease. Cyst development in ADPKD involves abnormal epithelial cell proliferation, which is affected by the primary cilia-mediated signal transduction in the epithelial cells. Thus, primary cilium has been considered as a therapeutic target for ADPKD. Since ADPKD exhibits many pathological features similar to solid tumors, we investigated whether targeting primary cilia using anti-tumor agents could alleviate the development of ADPKD. Twenty-four natural compounds with anti-tumor activity were screened in MDCK cyst model, and 1-Indanone displayed notable inhibition on renal cyst growth without cytotoxicity. This compound also inhibited cyst development in embryonic kidney cyst model. In neonatal kidney-specific *Pkd1* knockout mice, 1-Indanone remarkably slowed down kidney enlargement and cyst expansion. Furthermore, we demonstrated that 1-Indanone inhibited the abnormal elongation of cystic epithelial cilia by promoting tubulin polymerization and significantly down-regulating expression of anterograde transport motor protein KIF3A and IFT88. Moreover, we found that 1-Indanone significantly down-regulated ciliary coordinated Wnt/β-catenin, Hedgehog signaling pathways. These results demonstrate that 1-Indanone inhibits cystic cell proliferation by reducing abnormally prolonged cilia length in cystic epithelial cells, suggesting that 1-Indanone may hold therapeutic potential to retard cyst development in ADPKD.

Keywords: ADPKD; primary cilia; Cysts; 1-Indanone; anterograde transport motor protein

Acta Pharmacologica Sinica (2023) 44:406–420; https://doi.org/10.1038/s41401-022-00937-z

INTRODUCTION

Autosomal dominant polycystic kidney disease (ADPKD) is the most common inherited kidney disease, with a prevalence of 1/2500–1/1000 worldwide [1]. ADPKD is characterized by excessive proliferation of renal epithelial cells and progressive fluid-filled cysts in bilateral kidneys [2, 3], which is caused by mutations in *Pkd1* or *Pkd2* gene. *Pkd1* and *Pkd2* encode polycystin 1 (PC1) and polycystin 2 (PC2), respectively. PC1 and PC2 form a complex co-expressed on the primary cilia of renal tubular epithelial cells [4–6]. PC1 converts the mechanical signal alterations in cilia into intracellular calcium signal mediated by PC2 [7]. Defects of polycystin or primary cilia affect intracellular calcium and downstream signal transduction, which result in abnormal proliferation of renal tubular epithelial cells and secretion of cystic fluid, lead to the formation of renal cysts [8].

Most of ADPKD patients develop into end-stage renal disease around the age of 60 requiring kidney dialysis or transplantation [9], which imposes a serious burden to family and society [10, 11]. The clinical treatment of ADPKD is very limited. At present, there is only tolvaptan, a vasopressin type 2 receptor antagonist that is approved as a therapeutic medication for ADPKD [12–14]. However, the patients with long-term use of tolvaptan will face a high risk of liver injury [15–19]. Therefore, there is still an urgent need to discover therapeutic drugs that are effective against ADPKD with fewer adverse effects.

Intriguingly, ADPKD has extensive similar pathological features with solid tumors, including excessive cell proliferation, extracellular matrix remodeling, abnormal epithelial cellular polarity and differentiation, dysregulated energetics and alterations in primary cilia [20, 21].

Primary cilia are responsible for sensing fluid flow in eukaryotic cells, transducing extracellular mechanical and chemical signals into the cell and triggering physiological responses. When primary cilia are defective, they will lead to developmental disorders of various tissues and organs in the body, which are called ciliopathies.

The cystic kidney is the common phenotype in numerous ciliopathies. It is suggested that primary cilium defect may be an important trigger of the renal cyst formation [22]. Also, the abnormalities of primary cilia in renal tubular cells have been observed in many models of kidney disorders, indicating the central role of primary cilium in maintaining normal kidney function [23]. Previous study has found abnormalities in the primary cilium structure of renal epithelial cells in ADPKD [24].

[1]State Key Laboratory of Natural and Biomimetic Drugs, Department of Pharmacology, School of Basic Medical Sciences, Peking University, Beijing 100191, China; [2]Department of Anatomy, College of Basic Medicine, Chongqing Medical University, Chongqing 400016, China and [3]Key Laboratory of Molecular Cardiovascular Sciences, Ministry of Education, Beijing 100191, China
Correspondence: Bao-xue Yang (baoxue@bjmu.edu.cn)

Received: 24 January 2022 Accepted: 3 June 2022
Published online: 29 July 2022

Abnormal elongated primary cilia of cyst epithelial cells have been found in multiple PKD animal models such as *pcy*, *jck*, *Pkd1*$^{RC/RC}$, even in ADPKD patients [25–29]. Especially, abnormally elongated primary cilia were found in the early cystic stage of ADPKD patients. Primary cilium length is correlated with cyst expansion [30]. All these data indicate that primary cilia length is a critical factor of cyst development in ADPKD.

A study suggests that primary cilium functions as a therapeutic target for ADPKD, and targeting primary cilia assembly inhibits renal ciliogenesis [25]. However, there are still many controversies about the morphological and structural abnormalities of renal tubular cilia in different ADPKD models. And the mechanism of primary cilia in regulating renal cysts formation has not been clearly studied. Therefore, in this study we intended to investigate whether the development of ADPKD can be alleviated by directly targeting primary cilia by pharmacological approaches.

MATERIALS AND METHODS

Cell culture and CCK-8 assay

Madin-Darby Canine Kidney (MDCK) cells were cultured with Dulbecco's Modified Eagle's Medium (11965175, DMEM, Gibco, Waltham, MA, USA), and mouse inner medullary collecting duct (mIMCD-3) cells were cultured with Dulbecco's Modified Eagle's Medium/Nutrient Mixture F-12 (DMEM/F12, 12400024, Gibco, Waltham, MA, USA). They were cultured in DMEM/F-12 with 10% fetal bovine serum (FBS, 10099141C, Gibco, Waltham, MA, USA), 100 μg/ml streptomycin, and 100 U/ml penicillin, incubated at 37 °C with 5% CO_2. MDCK cells were seeded on a 96-well plate at a density of 5000 cells/well. After treatment with candidate compounds at 25 μM for 24 h, 100 μl 5% CCK-8 solution (CK04, Dojindo Molecular Technologies, Kumamoto, Japan) was added to each well and incubated for 2 h. Absorbance at 450 nm was measured with a microplate reader (MQX200, Biotek, Winooski, VT, USA). When reached to 70% density, mIMCD cells were incubated with 10 μM of forskolin (FSK, 66575-29-9, Sigma, Saint Louis, MO, USA) for 0.5 h or 3 h and treated with different concentrations of 1-Indanone.

MDCK cyst model

MDCK cells were digested and resuspended in type I collagen (C2124, Sigma, Saint Louis, MO, USA) solution containing modified Eagle's medium and 10 mM HEPES at pH~7.2. The cell suspensions were allocated into 24-well plates and cultured with DMEM-F12 medium with 10% FBS. FSK was supplemented from day 5 to stimulate cysts formation. Medium was changed every 12 h. Cysts were tracked by taking photos (30 cysts/well) every 2 days from day 4 to record their growth curve. Cyst diameter was measured and analyzed with ImageJ software (NIH Image, Bethesda, MD, USA). To assay cyst formation, the numbers of cysts and colonies were counted at day 6 of incubation with the test compounds.

Embryonic kidney cyst model

Embryonic kidney cyst model was set up as described [31]. Briefly, embryos at day 13.5 were harvested from pregnant ICR mice. Embryonic kidneys were placed on transwell filters (CLS3401-48EA, Corning, NY, USA) filled with conditioned medium as described. DMEM-F12 supplemented with 2 mM *L*-glutamine, 250 U/ml penicillin, 250 μg/ml streptomycin, 10 mM HEPES, 5 μg/ml insulin, 5 μg/ml transferrin, 2.8 nM selenium, 25 ng/ml prostaglandin E1, 32 pg/ml T3, and 100 μM 8-bromoadenosine-3',5'-cyclic monophosphate (8-Br-cAMP, 23583-48-4, Sigma, MO, USA). Test compounds were supplemented from day 0 and medium was changed every 12 h. Through 6 days culture, embryonic kidney cysts grew massively under stimulation of 100 μM 8-Br-cAMP. The kidney micrographs were tracked on day 0, 2, 4, and 6. Cystic area and total kidney area were analyzed using ImageJ software (NIH Image, Bethesda, MD, USA).

Mouse model

Pkd1$^{flox/flox}$*: Ksp-Cre* mice (C57BL/6 genetic background) were generated by intercrossing *Pkd1*$^{flox/+}$ mice (from the laboratory of Dr. Stefan Somlo) with *Ksp-Cre* transgenic mice (from the laboratory of Dr. Peter Igarashi). Genotyping was conducted on postnatal day 1. From postnatal day 1 to day 5, mice were injected with candidate compound at 100 mg·kg^{-1}·d^{-1} or vehicle solution subcutaneously. Mice were sacrificed on postnatal day 5. All experiments conducted on animals were according to animal protocols approved by the Peking University Health Science Center Committee on Animal Research (26 Febrary 2021; protocol no. LA2021080).

Molecular docking studies

1-Indanone was drawn in "ChemBioDraw Ultra" 14.0, transformed to 3D conformations and minimized using the "LigPrep" module in "Schrödinger 2018". Microtubule (PDB code: 6EW0) was prepared for docking using the "Protein Preparation" module, and a grid box was created using "Receptor Grid Generation". Prepared 1-Indanone was docked with microtuble using "Ligand Docking". Bound complexes were visualized in "Schrödinger 2018".

Measurements of cilium length

Imaging and quantification of cilium length was performed using the Galvano scanner of a Nikon A1+ confocal Ti microscope system with a ×100 immersion objective lens and ×4 optical zoom. Primary cilia were acquired from a minimum of 50 cells for each group and cilium length was measured using the "*z* projection" function of ImageJ software (NIH Image, Bethesda, MD, USA). The distance from the base to the tip of the cilium was measured by tracing the length of the cilium, using ImageJ's segmented line tool. The cilium length of renal tubules or cysts was measured manually using ImageJ software (NIH Image, Bethesda, MD, USA) and converted in micrometers (0.031 μm/pixel).

Tubulin isolation and purification

Microtubule protein was purified from porcine brain by three cycles of temperature-dependent assembly and disassembly in buffer A (0.1 M Pipes, 2 mM EGTA, 1 mM $MgSO_4$, pH 6.4) as described [32]. The first polymerization step was carried out in the presence of 4 M glycerol and the two further polymerization steps were performed without glycerol. Microtubule protein was stored at −70 °C in buffer A at a protein concentration of ~15–20 mg/ml.

Tubulin polymerization assay

Tubulin was reconstituted to 3 mg/ml using G-PEM buffer. The tubulin (100 μl) was added to each well of a pre-warmed 96-well plate and exposed to test compounds at 25 μM. The absorbance at 340 nm was recorded every 1 min for 65 min using a TECAN GENios multifunction microplate reader (IC 12833, TECAN U.S. Inc., Research Triangle Park, NC, USA) at 37 °C. The dose-response curves were plotted using Graphpad Prism (Graphpad Software Inc., San Diego, CA, USA).

Western blot

Proteins were separated on SDS-polyacrylamide gel though electrophoresis and then transferred to polyvinylidene difluoride membranes (IPVH00010, Millipore, Saint Louis, MO, USA). After blocking with 5% bovine serum albumin for 2 h at room temperature, membranes were incubated with primary antibodies (Table 1) overnight at 4 °C. Membranes were washed and incubated with goat anti-mouse IgG or goat anti-rabbit IgG secondary antibodies for 1 h at room temperature. Blots were then developed with the ECL kit (BF06053S-100, Biodragon, Suzhou, China) and detected with a chemiluminescence detection system (GeneGnomeXRQ, Syngene, Cambridge, United Kingdom). The expression levels of proteins were quantified relative to β-actin expression.

Table 1. Antibody information.

Antigen	Manufactor	CAS	RRID	Dilution
PCNA	Cell Signaling Technology	2586	AB_2160343	1:2000
H-ras	Proteintech	18295-1-AP	AB_2121046	1:1000
B-raf	Proteintech	20899-1-AP	AB_2878760	1:1000
p-ERK	Cell Signaling Technology	4370	AB_2315112	1:2000
ERK1/2	Cell Signaling Technology	9102	AB_2814870	1:1000
active β-catenin	Cell Signaling Technology	8814	AB_11127203	1:1000
β-catenin	ABclonal	A11512	AB_2814869	1:1000
cyclin D1	Bioworld	BS2436	AB_1662130	1:1000
c-myc	Cell Signaling Technology	9402	AB_2151827	1:1000
p-gsk3β	Cell Signaling Technology	9336	AB_331405	1:1000
gsk3β	Cell Signaling Technology	12456	AB_2636978	1:1000
p-mTOR	Cell Signaling Technology	2971	AB_330970	1:1000
mTOR	Cell Signaling Technology	2972	AB_330978	1:1000
p-p70S6K	Cell Signaling Technology	9025	AB_2734746	1:1000
p70S6K	Proteintech	14485-1-AP	AB_2269787	1:1000
p-S6	ABclonal	AP0537	AB_2771524	1:1000
S6	ABclonal	A6058	AB_2766731	1:1000
GLI1	Proteintech	66905-1-AP	AB_2882232	1:1000
GLI2	Proteintech	18989-1-AP	AB_10596479	1:1000
GLI3	Proteintech	19949-1-AP	AB_11182281	1:1000
IFT88	Proteintech	13967-1-AP	AB_2121979	1:1000
ARL13B	Thermo Fisher Scientific	PA5-92354	AB_2806450	1:1000
KIF3A	Santa Cruz Biotechnology	sc-376680	AB_11149751	1:1000
KIF3B	Santa Cruz Biotechnology	sc-50456	AB_2132068	1:1000
KIF17	Santa Cruz Biotechnology	sc-393253	AB_2131285	1:1000
Alpha-tubulin (acetyl K40)	Abcam	ab179484	AB_2890906	1:1000
β-actin	ABclonal	AC026	AB_2768234	1:20000
Fluorescein (FITC)-conjugated affinipure goat anti-mouse IgG (H + L)	Proteintech	SA00003-1	AB_2890896	1:800
Fluorescein (FITC)-conjugated affinipure goat anti-rabbit IgG (H + L)	Proteintech	SA00003-2	AB_2890989	1:800
Cy3-conjugated affinipure goat anti-rabbit IgG (H + L)	Proteintech	SA00009-2	AB_2890957	1:800

Histological staining and immunofluorescence staining

For hematoxylin and eosin (H&E) and Masson's trichome staining, 5 μm of kidney paraffin sections were used. Cyst diameter and cystic index were calculated using ImageJ software (NIH Image, Bethesda, MD, USA). Cystic area was measured based on the definition that a cyst has spherical structure with diameter ≥ 50 μm (cyst index = total cystic area/total kidney area) × 100%. For immunofluorescence staining, sections were blocked with 5% (w/v) goat serum at room temperature for 1 h and then incubated with a primary antibody for Ki-67 (Abcam, Cat# ab15580, RRID: AB_443209, 1:500 dilution), anti-ARL13B (Thermo Fisher Scientific, Cat# PA5-92354, RRID: AB_2806450, 1:200 dilution) at 4 °C overnight. After washing three times, sections were incubated with secondary antibody or *Lotus tetragonolobus* lectin (LTL, Vector Laboratories, Cat# FL-1321, RRID: AB_2336559, 1:400 dilution) and *Dolichos biflorus* agglutinin (DBA, Vector Laboratories, Cat# RL-1032, RRID: AB_2336396, 1:400 dilution) for 1 h. Hoechst dye (Sigma Aldrich, Cat# 94403, 1:1000 dilution) was used to stain nuclei. All images were captured with a Nikon fluorescence microscope.

Scanning electronic microscope (SEM)

The kidneys of mice were perfused and fixed as described [33]. One cubic millimeter tissues were collected and stored in fixative (2% glutaraldehyde in 0.1 M cacodylate buffer, pH range 6.8–7.4) for 24 h at 4 °C. Then, tissues were subsequently washed with PBS three times. The samples were kept in 1% osmium tetroxide fixative for 3 h. The samples were rinsed with distilled water. The processed tissues were dehydrated in different concentration of ethanol: 50%, 70%, 95%, and 100% with each step for 10–20 min. And the tissue samples were mounted onto metal stubs and coated with gold. Samples were viewed using a Hitachi tm4000 plusII (Hitachi, Tokyo, Japan) scanning electron microscope.

Transmission electronic microscope (TEM)

For TEM, tissue samples were fixed and dehydrated same as SEM. The samples were then transferred to embedding resin in acetone. Small pieces of kidney were embedded with TEM of epoxy resin embedded tissue kit (Genmed Gene Pharmaceutical Co., Ltd, Shanghai, China). Semithin sections were cut with a LKB III ultratome, and stained with the electron dense agent uranyl acetate and lead citrate to provide contrast. Staining was achieved by floating grids specimen side down on a small drop of stain on a piece of Parafilm, with extensive washing with distilled water after each step. Then ultrathin sections were ready for viewing and capturing.

Statistical analysis

All results were analyzed with GraphPad Prism software and expressed as mean values ± SEM. Statistics were analyzed by Student's *t* test or one-way ANOVA followed by the Tukey's

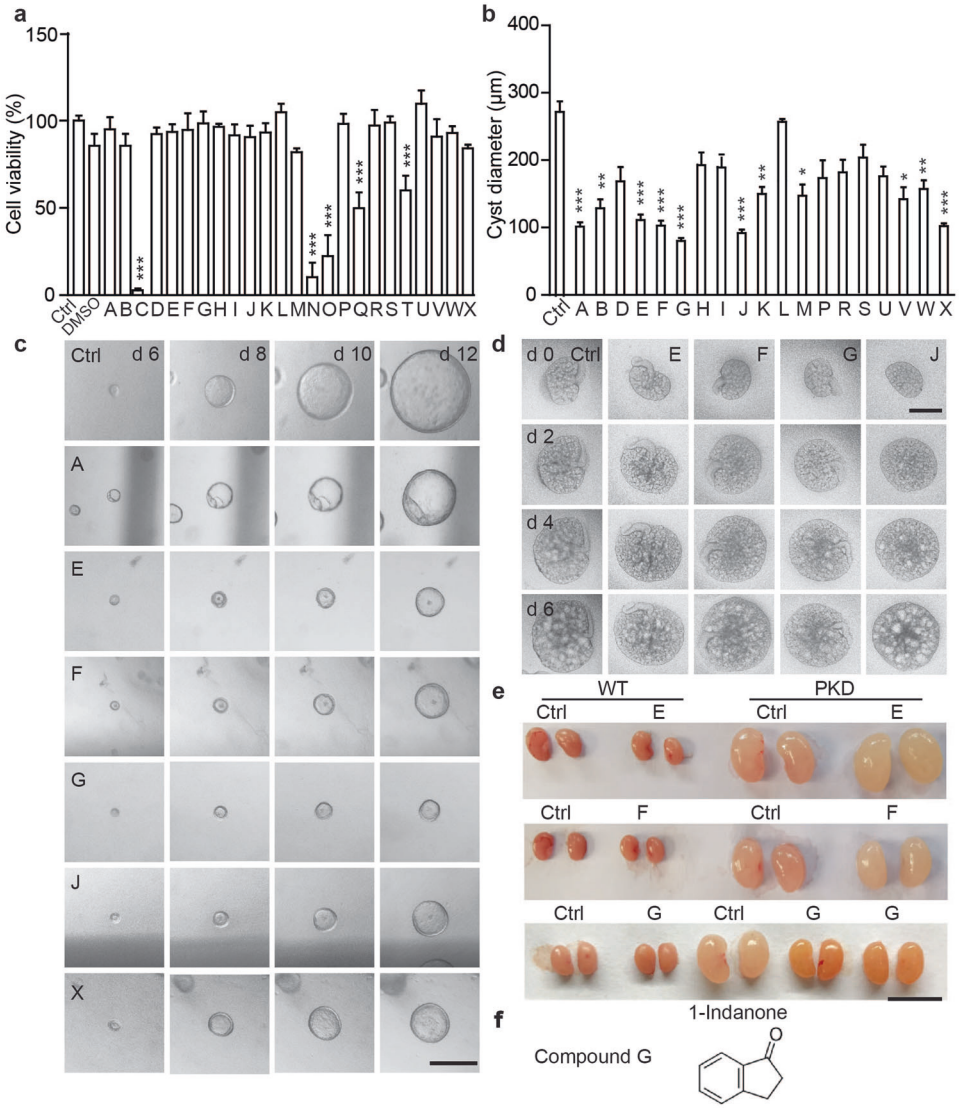

Fig. 1 1-Indanone is identified as an inhibitor of renal cysts. a Cell viability examined by CCK-8. $n = 6$. **b** Cyst inhibition activity of tested compounds in MDCK cyst model. $n \geq 30$. **c** Representative micrographs of MDCK cysts treated with compounds A, E, F, G, J, and X. Bar = 200 μm. **d** Representative micrographs of embryonic kidneys treated with compounds E, F, G, and J. Bar = 1 mm. **e** Representative photographs of wild-type (WT) and *Pkd1* knockout (PKD) kidneys treated with compounds E, F, and G. Bar = 1 cm. **f** The chemical structure of 1-Indanone (compound G). Data are presented as means ± SEM. $^{*}P < 0.05$, $^{**}P < 0.01$, $^{***}P < 0.001$ vs. Ctrl group.

multiple comparison tests was performed in. P value < 0.05 was considered statistically significant in all tests.

RESULTS

1-Indanone was found to inhibit cyst development

Twenty-four compounds were virtually screened from the natural compound library (from Targetmol Biochemical) based on their inhibitory activity on cell proliferation signaling, such as Ras/MAPK, mTOR and Wnt signaling pathways. Compounds C, N, O, Q, T were excluded due to their cytotoxicity on MDCK cells by CCK-8 assay (Fig. 1a). The inhibitory activity on cysts of 19 remainders was determined in MDCK cyst model. The experimental results showed that compounds A, E, F, G, J, X remarkably inhibited the enlargement of MDCK cysts (Fig. 1b, c). The active compounds E, F, G, and J with the remarkable inhibitory effect on MDCK cyst were selected for further investigation in the embryonic kidney cyst model. Compounds E, F and G markedly suppressed the cyst expansion of embryonic kidney and reduced the cyst index without effect on kidney development (Fig. 1d). However, in the kidney-specific *Pkd1* knockout (*Pkd1*$^{flox/flox}$*: Ksp-Cre*) mouse model, only compound G showed notable inhibition on the development of renal cysts (Fig. 1e). These data suggested that compound G, which chemical name is 1-Indanone (Fig. 1f), had an inhibitory effect on cysts and was conducted in further pharmacological and mechanistic studies.

1-Indanone was pharmacologically confirmed to suppress cyst development

Further, we adopted *Pkd1*$^{flox/flox}$; *Ksp-Cre* mice to test the inhibitory effect of 1-Indanone on renal cysts in vivo. From postnatal day 1 to day 5, *Pkd1* knockout (PKD) mice were subcutaneously injected with 1-Indanone at 25, 50 or 100 mg·kg^{-1}·d^{-1} or vehicle solution. There was no notable difference in appearance (Fig. 2a), body weight (Fig. 2b) or the liver index (Fig. 2c) between mice with or without 1-Indanone treatment. The organ indexes of brain, heart and gut in the mice of each group indicated 1-indanone had no obvious toxicity in vivo (data not shown). The kidney volume of

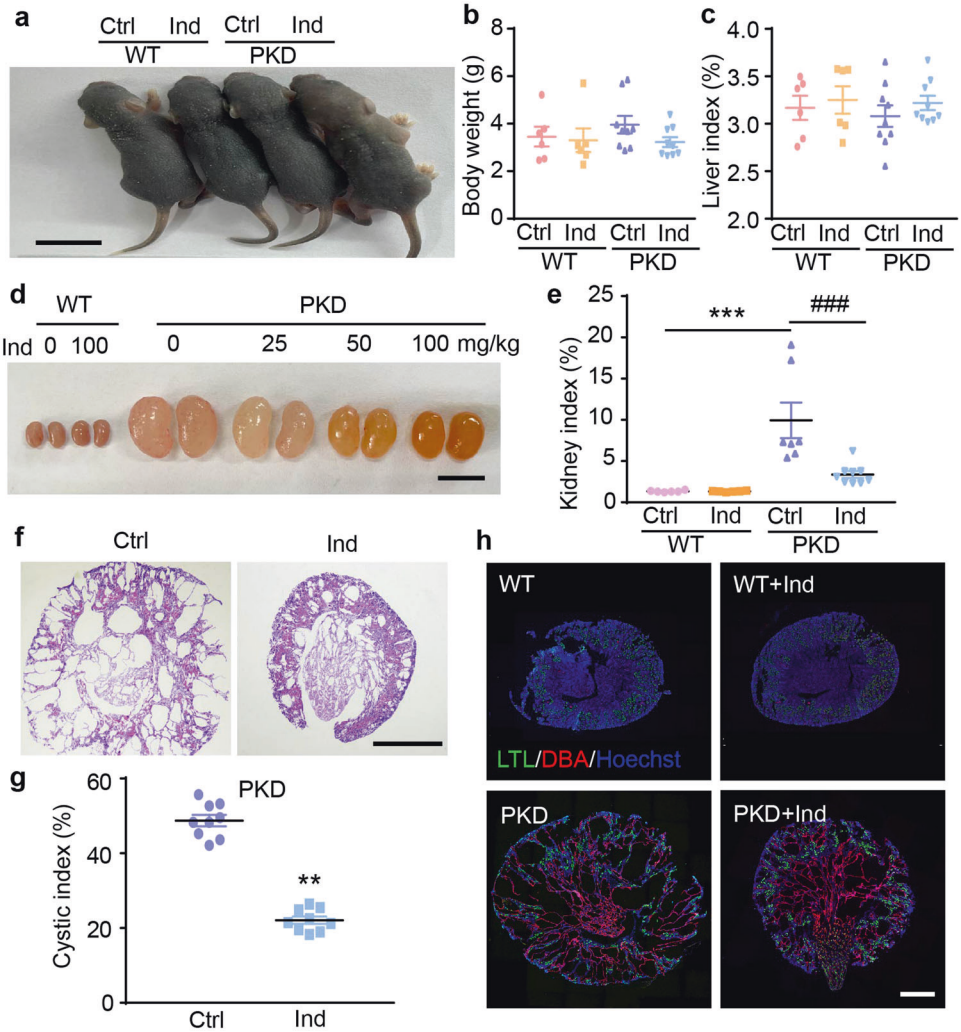

Fig. 2 1-Indanone suppresses cyst expansion in PKD mice. a Representative photographs of wild-type (WT) and *Pkd1* knockout (PKD) mice treated without (Ctrl) or with 1-Indanone (Ind) at 100mg·kg^{-1}·d^{-1}. Bar = 2 cm. **b** Body weight. $n \geq 6$. **c** Liver index (percentage of liver weight to body weight). $n \geq 6$. **d** Representative photographs of WT and PKD kidneys treated without or with 1-Indanone at 25, 50, 100 mg·kg^{-1}·day^{-1} from postnatal day 1 to day 5. Bar = 1 cm. **e** Kidney index (percentage of kidney weight to body weight) of WT and PKD mice treated with 1-Indanone at 100 mg·kg^{-1}·d^{-1}. $n \geq 6$. $^{***}P < 0.001$ vs. Ctrl group in WT mice. $^{\#\#\#}P < 0.001$ vs. Ctrl group in PKD mice. **f** Representative kidney sections with H&E staining from PKD mice treated with vehicle (left) or with 1-Indanone (right) (100 mg·kg^{-1}·d^{-1}). Bar = 500 μm. **g** Cystic index (percentage of cystic area to whole kidney area). $n = 9$. $^{**}P < 0.01$ vs. Ctrl group in PKD mice. **h** Immunofluorescence staining of LTL and DBA on kidney sections from WT or PKD mice treated without or with Ind. Bar = 1 mm. All data are presented as mean values ± SEM.

PKD mice was dose-dependently decreased under the treatment with 1-Indanone at 25, 50, or 100 mg·kg^{-1}·d^{-1} (Fig. 2d) and the kidney index of PKD mice was pronouncedly reduced by 1-Indanone at 100 mg·kg^{-1}·d^{-1} (Fig. 2e). Kidney sections stained with H&E showed that cystic area in PKD kidneys was conspicuously reduced by 1-Indanone at 100 mg·kg^{-1}·d^{-1} (Fig. 2f, g). The immunostaining results of LTL and DBA revealed that 1-Indanone mainly inhibited the expansion of cysts derived from the collecting duct in PKD mice (Fig. 2h).

To determine whether 1-Indanone could affect cyst formation, we examined the effect of 1-Indanone on MDCK cyst model. MDCK cells were cultured in 3D collagen gel with FSK (10 μM) for 6 days without or with 1-Indanone. The statistic results showed that 25 μM of 1-Indanone notably reduced the number of MDCK cysts without affecting the number of total cell colonies (Fig. 3a), which indicated 25 μM of 1-Indanone inhibited MDCK cyst formation. For assaying the effect of 1-Indanone on the enlargement of MDCK cyst, MDCK cells were cultured in 3D collagen gel with 10 μM FSK for 4 days. Then the MDCK cysts were treated with 1-Indanone at 1, 5 or 25 μM from day 5 to day 12. The MDCK cysts treated with FSK alone were enlarged excessively with diameters around 350 μm on day 12 (Supplementary Fig. S1). The enlargement of MDCK cysts was suppressed with 1-Indanone in a dose-dependent manner (Fig. 3b). We further investigated whether the inhibitory effect of 1-Indanone is reversible. After 1-Indanone was washed out on day 8, the cysts were re-enlarged with FSK stimulation, suggesting the inhibitory effect of 1-Indanone is reversible (Fig. 3c).

The reversibly inhibitory effect of 1-Indanone was confirmed in embryonic kidney cyst model. E13.5 embryonic kidneys were stimulated by 100 μM 8-Br-cAMP for 6 days without or with 1-Indanone treatment for 4 days. The experimental results showed that 8-Br-cAMP-induced cyst expansion in embryonic kidneys was markedly retarded by 25 μM 1-Indanone (Fig. 3d, e). However, after 1-Indanone was washed out on day 4, renal cysts regrew progressively, which indicated that 1-Indanone reversibly inhibited cyst development in embryonic kidneys.

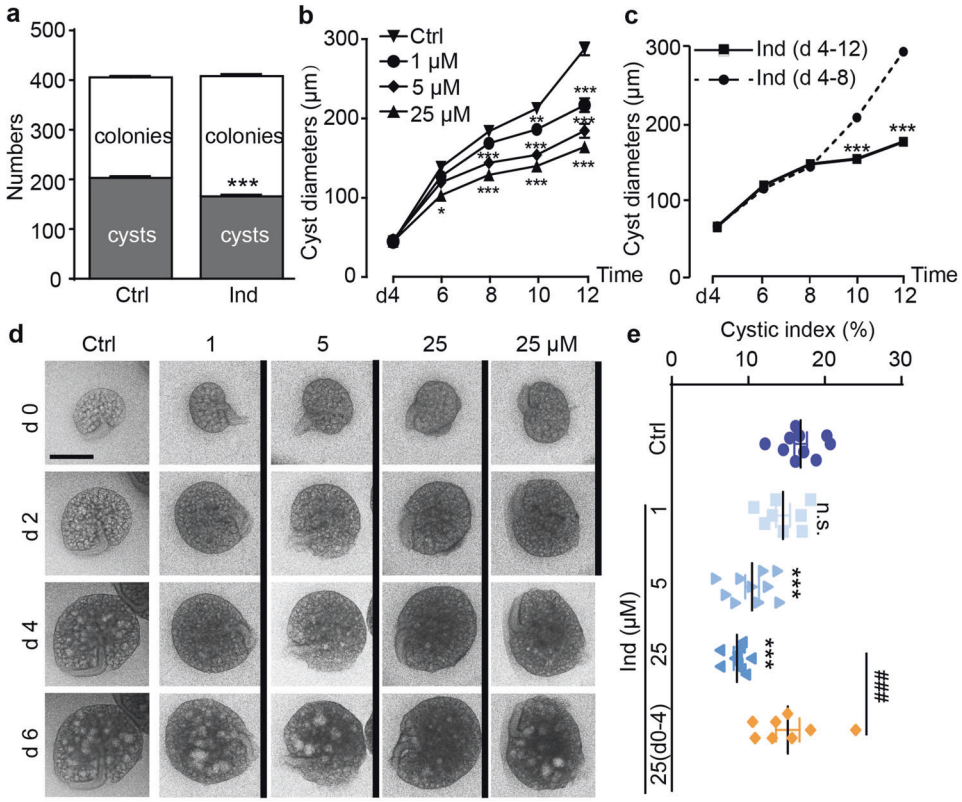

Fig. 3 1-Indanone retards cyst progression dose-dependently. a Numbers of total colonies and MDCK cysts treated without (Ctrl) or with 25 μM of 1-Indanone (Ind) for 6 days. $n = 10$. **b** Growth curves of MDCK cysts treated with Ind at 1, 5, 25 μM. $n = 50$ in each group. **c** Growth curves of MDCK cysts treated with 25 μM 1-Indanone from day 4 to day 12 (solid line) or from day 4 to day 8 (dashed line). $n = 50$. **d** Representative micrographs of embryonic kidneys treated with 1-Indanone. Bar = 1 mm. Black lines means the time of 1-Indanone treatment. **e** Cyst index of embryonic kidneys treated with 1-Indanone at 1, 5, 25 μM for 6 days or 25 μM for 4 days. $n \geq 8$. Data are presented as mean values ± SEM. Data are analyzed with one-way ANOVA multiple comparisons. $^{*}P < 0.05$, $^{**}P < 0.01$, $^{***}P < 0.001$ vs. Ctrl group. $^{\#\#\#}P < 0.001$ vs. the group treat with 25 μM 1-Indanone for 6 days.

1-Indanone inhibited hyperproliferation of cystic epithelial cells

Hyperproliferation of cystic epithelial cells is the main pathological feature of ADPKD. Immunofluorescence showed that the number of Ki67-positive cells in the kidneys of PKD mice was significantly reduced after 1-Indanone treatment (Fig. 4a). Consistently, the up-regulated PCNA, a proliferation marker protein, was remarkably suppressed by 1-Indanone in PKD kidneys (Fig. 4b). In order to further verify the effect of 1-Indanone on cell proliferation, we detected the activation of cAMP response element binding protein (CREB) and Ras/MAPK and mTOR signaling pathways, which play critical roles in regulating cellular over-proliferation in ADPKD [34]. It was found that 1-Indanone inhibited the excessive activation of the CREB and ERK in Ras/MAPK signaling pathway. The expression of H-ras and B-raf tended to be down-regulated by 1-Indanone, but there was no statistical difference (Fig. 4c and Supplementary Fig. S2a). Moreover, the expression and activation of mTOR, S6K, S6 in mTOR signaling pathway in PKD mice were also retarded after 1-Indanone treatment (Fig. 4d and Supplementary Fig. S2b). These results indicated that 1-Indanone inhibited the cellular hyperproliferation in PKD by mTOR and MAPK pathways.

1-Indanone inhibited the abnormally elongation of primary cilia in cystic epithelium

It is well established that the defects in the structure of primary cilia are related to renal cyst development [35]. There is evidence proved that primary cilia length in cystic epithelial cells correlated with ADPKD progression [30]. Therefore, we investigated the structural change of the primary cilia of renal tubular epithelial cells in PKD mice and the effect of 1-Indanone on primary cilia. Immunofluorescence staining with ARL13B showed that the lengthes of primary cilia in cystic and tubular epithelial cells of PKD mice were abnormally increased (Fig. 5a). 1-Indanone notably inhibited the abnormal elongation of primary cilia in PKD kidney cystic epithelial cells, and had no notable effect on that in wild-type kidneys. We further observed the structure of primary cilia using transmission electronic microscope (TEM) and scanning electronic microscope (SEM). Consistent with immunofluorescence results, TEM and SEM images also showed that primary cilia were abnormally lengthened and thinner in PKD kidneys, which were inhibited by 1-Indanone (Fig. 5b, c).

To confirm the effect of 1-Indanone on primary cilia length, we stimulated mIMCD cells with cAMP agonist FSK and detected primary cilia by immunofluorescence staining with ARL13B. Consistent with the results of PKD mice, after stimulation with 100 μM FSK for 3 h, the primary cilia of mIMCD cells were prolonged excessively, even reaching 2-fold of those in the ctrl group (Fig. 6a). Studies have confirmed that activation of mTORC1 or PKA will promote the elongation of primary cilia [36, 37], therefore mTORC1 inhibitor rapamycin and PKA inhibitor H-89 were used as positive controls in this study. It was found that 1-Indanone remarkably inhibited the excessive elongation of cilia by cAMP activation in mIMCD cells, similar to the effect of rapamycin (Fig. 6a) or H-89 (Fig. 6b). There was no significant difference in the length of primary cilia in mIMCD cells without and with 1-Indanone treatment (Fig. 6a, b). In addition, we detected the effect of 1-Indanone on the ciliary basal body by gamma-tubulin immunofluorescence staining. There was no difference in the structure of the ciliary basal

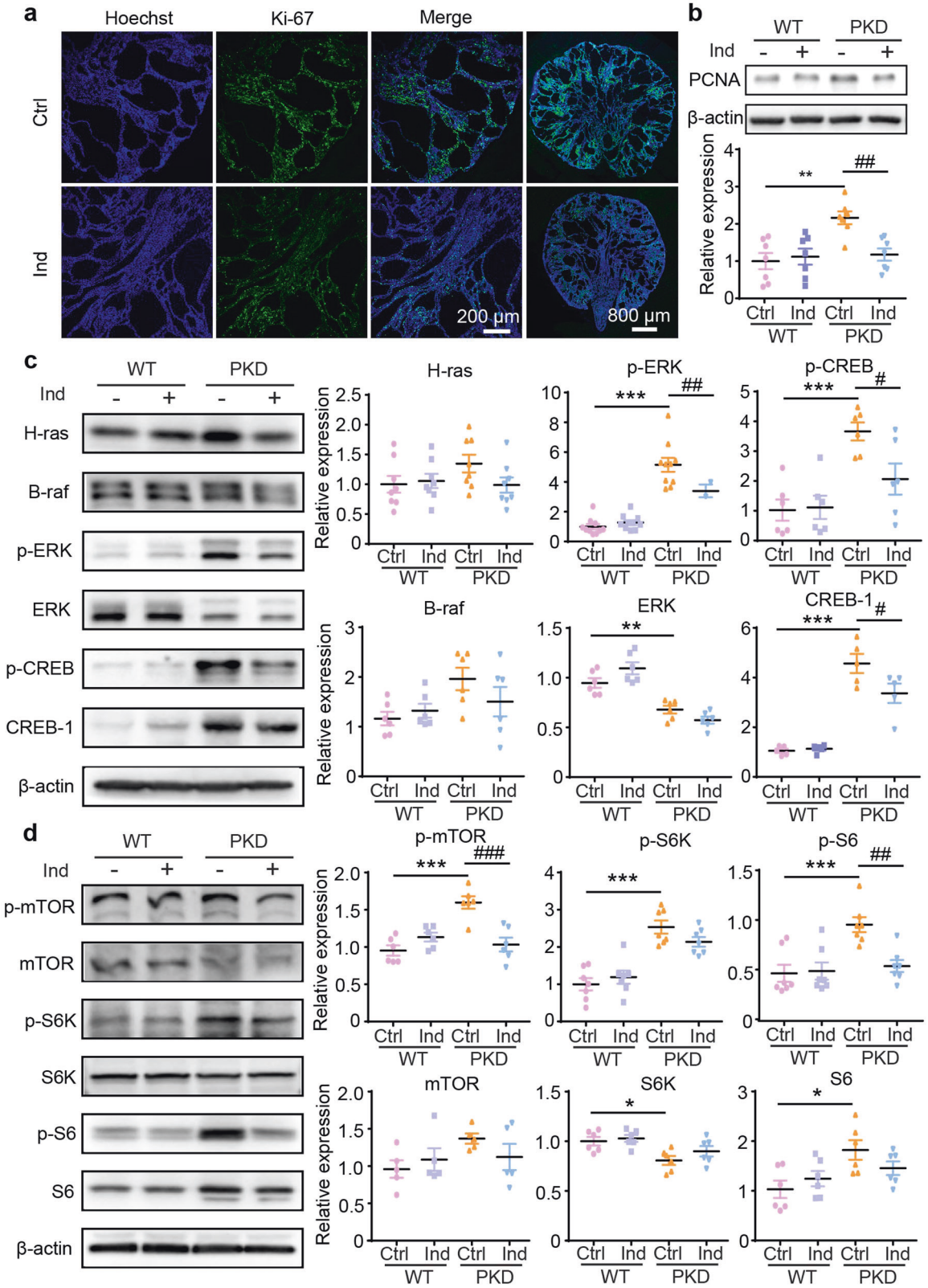

Fig. 4 1-Indanone inhibits abnormal cell proliferation in PKD mice. a Representative immunofluorescence images of the kidney sections stained with Ki-67 in PKD mice without (Ctrl) or with 1-Indanone (Ind) treatment. Magnification bar = 200 μm. Bar = 800 μm. **b** Representative Western blots (upper) and relative protein expression (lower) of PCNA in kidneys of PKD and wild-type (WT) mice treated without or with 1-Indanone at 100 mg· kg^{-1}·d^{-1} for 4 days. $n = 7$. **c** Representative Western blots (left) and relative protein expression (right) of proteins in Ras/MAPK signaling pathway in the kidneys of WT mice and PKD mice without or with 1-Indanone treatment. $n \geq 6$. **d** Representative Western blots (left) and relative protein expression (right) of proteins in mTOR signaling pathway in the kidneys of WT mice and PKD mice with vehicle or 1-Indanone treatment. $n \geq 6$. Data are presented by mean values ± SEM. $^{*}P < 0.05$, $^{**}P < 0.01$, $^{***}P < 0.001$ vs. Ctrl group in WT mice, $^{\#}P < 0.05$, $^{\#\#}P < 0.01$, $^{\#\#\#}P < 0.001$ vs. Ctrl group in PKD mice. Data are analyzed with one-way ANOVA.

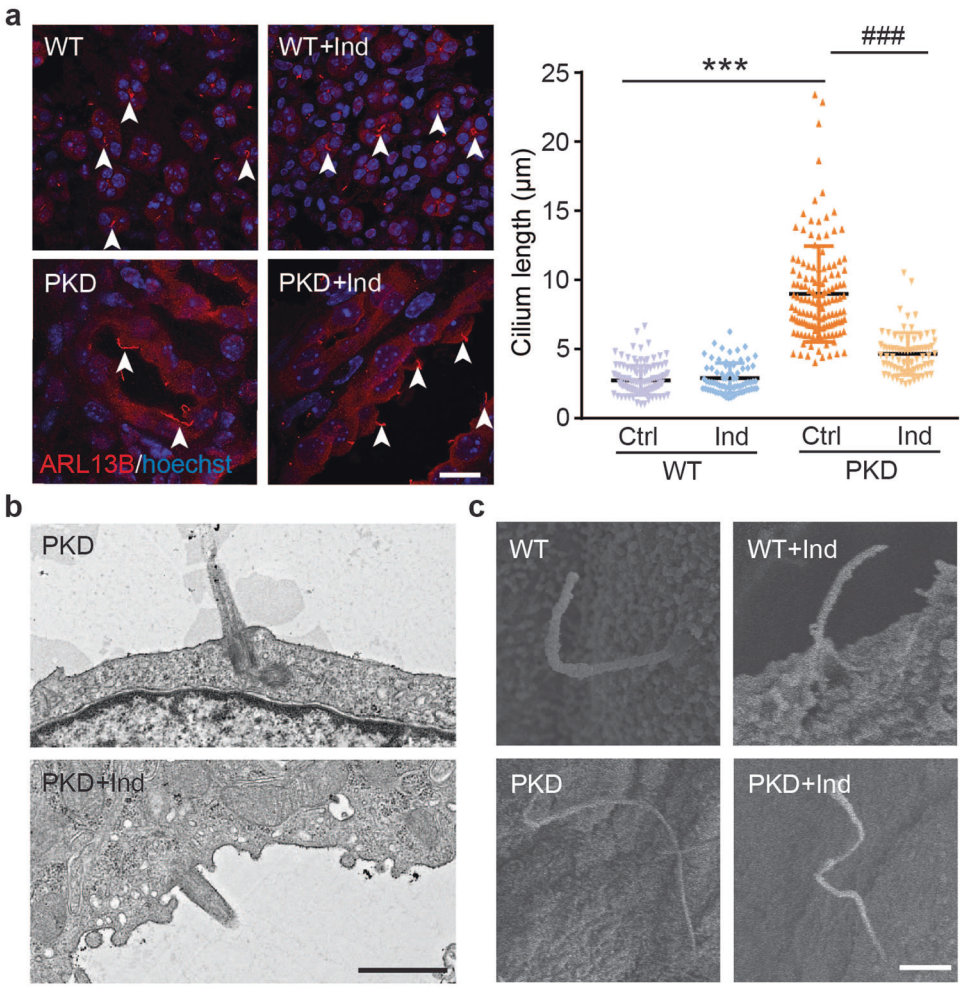

Fig. 5 1-Indanone reduces the primary cilium length of renal tubular epithelium in PKD mice. a Representative immunofluorescence images (left) and length of primary cilia in tubular and cystic epithelial cells in kidneys of PKD mice treated without (Ctrl) or with 1-Indanone (Ind) (right). Bar = 20 μm. $n > 60$, in three mice of each group. Data are presented by mean values ± SEM. Data are analyzed with one-way ANOVA. $^{***}P < 0.001$ vs. Ctrl group in WT mice, $^{###}P < 0.001$ vs. Ctrl group in PKD mice. **b** Representative TEM images of primary cilia in PKD mice treated without or with Ind. Bar = 1 μm. **c** Representative SEM images of primary cilia in each group. Bar = 1 μm.

body between 1-Indanone-treated group and the other groups in mIMCD cells (Supplementary Fig. S3), which indicated ciliary structural integrity was not disrupted by 1-Indanone.

These results demonstrated that 1-Indanone inhibited the elongation of the primary cilia caused by activation of PKA and cAMP in tubular epithelial cells.

1-Indanone inhibited excessive elongation of primary cilia in PKD by stabilizing tubulin

As the principal component of ciliated axoneme, microtubule dynamics directly modulate the cilia assembly [38]. Therefore, we explored whether modulating cilia length by 1-Indanone is associated with changes in tubulin dynamics. Virtual docking model showed 1-Indanone forms a hydrogen bond with arginine 359 in the paclitaxel binding site of tubulin (PDB ID: 6EW0) (Fig. 7a). Immunofluorescence staining results showed 25 μM of 1-Indanone promoted tubulin accumulation around the nucleus (Fig. 7b). We further detected the effect of 1-Indanone on tubulin polymerization. The absorbance at 340 nm of tubulin showed 25 μM of 1-Indanone promoted tubulin polymerization (Fig. 7c). These results indicated that 1-Indanone inhibited the abnormal elongation of primary cilia through tubulin stabilization. As the key component of the spindle apparatus, microtubule participates in mitosis regulating the cell cycle [39]. Therefore, we tested the effect of 1-Indanone on the cell cycle of mIMCD cells with or without FSK stimulation. It was found that FSK stimulation increased the number of mIMCD cells in G_0/G_1 phases, and the cells in S and G_2 phases were decreased compared with ctrl group. 1-Indanone inhibited the increased FSK-treated mIMCD cells in G_0/G_1 phases, but had no obvious effect on the cell cycle of those in the ctrl group (at least at the concentration we tested) (Supplementary Fig. S4).

1-Indanone down-regulated the anterograde transport of primary cilia in PKD mice

Cilia assembly and disassembly were determined by anterograde or retrograde transport process. The elongation of cilia relies on the anterograde intraflagellar process regulated by IFT-B and kinesin II [40]. Therefore, we detected the expressions of critical components of IFT-B and kinesin II, IFT88, KIF3A and KIF3B. The results showed that the expression of IFT88 was up-regulated impressively in PKD kidneys, which was retarded by 1-Indanone (Fig. 8a). And 1-Indanone notably reversed the abnormal up-regulation of both KIF3A and KIF3B in PKD kidneys (Fig. 8b, c), demonstrating 1-Indanone affected cilium assembly through down-regulating ciliary anterograde IFT progress.

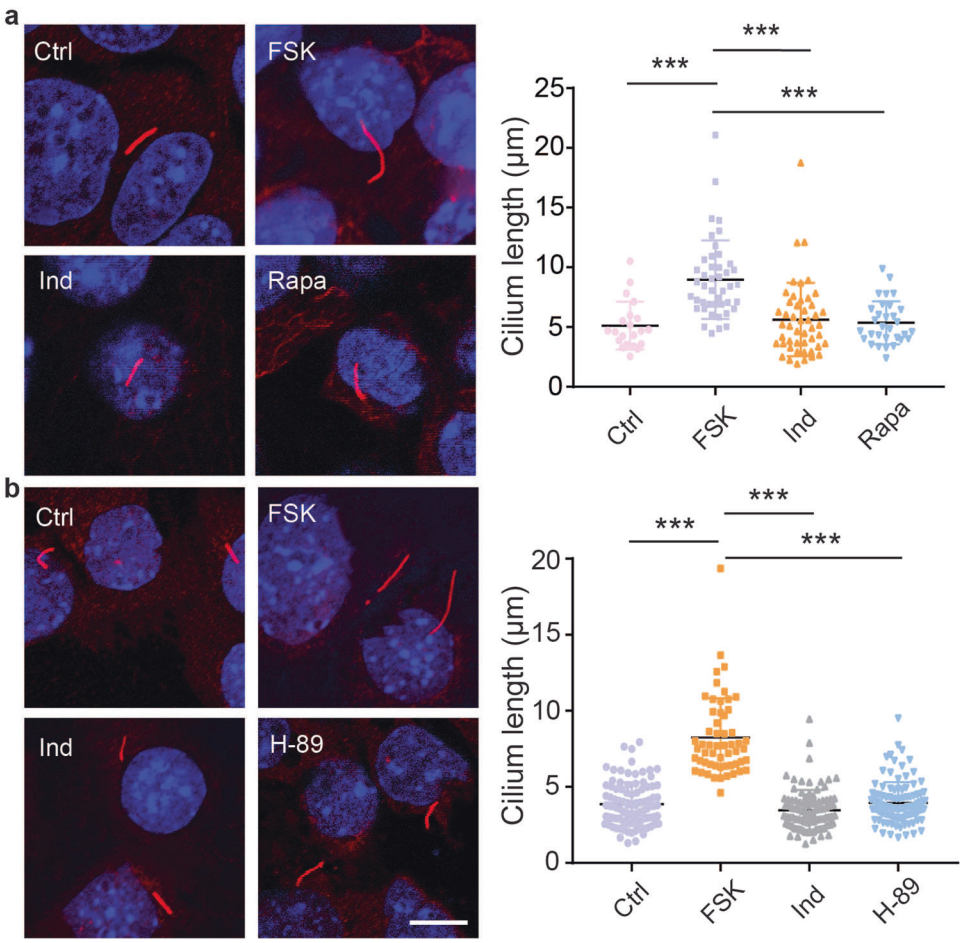

Fig. 6 1-Indanone retards primary cilia prolongation with FSK stimulation in mIMCD cells. a Representative image of primary cilium and quantification results of cilium length in mIMCD cells (Ctrl) or forskolin stimulated (FSK, 100 μM) mIMCD cells incubated with 1-Indanone (Ind, 25 μM) or rapamycin (Rapa, 20 nM), respectively. $n = 39–98$ in each group. Bar = 10 μm. ***$P < 0.001$. **b** Representative image of primary cilium and quantification results of cilium length in mIMCD ctrl cells or FSK-stimulated mIMCD cells incubated with 1-Indanone (Ind, 25 μM) or H-89 (10 μM), respectively. $n > 60$ in each group. Bar = 10 μm. Data are presented by mean values ± SEM. ***$P < 0.001$. Data are analyzed with one-way ANOVA.

We further detected the expression of IFT20, another subunit of IFT-B, which regulates primary cilia growth as well [41]. The results showed consistent with IFT88, the expression of IFT20 was markedly increased in PKD kidneys and was inhibited by 1-Indanone. Another motor protein in kinesin II, KIF17, has been reported to alter the dynamics of microtubules by promoting its polymerization. We found that the expression of KIF17 was reduced in PKD, and 1-Indanone had no notable effect on its expression (Fig. 8d).

The ciliary membrane protein Arl13b was reported to regulate cilia length by inducing cilia protrusion [42, 43]. And acetylated tubulin modulates cilia length by regulating cilia axoneme extension [44]. However, there was no notable difference in the expression of ARL13B and acetylated tubulin among each group, suggested that 1-Indanone does not affect the extension of ciliary membranes and axoneme by affecting the modification of microtubule (Supplementary Fig. S5).

1-Indanone down-regulated the ciliary coordinated signaling pathways

Above results have confirmed that 1-Indanone modulates the primary cilium structure, however it is unclear whether 1-Indanone affects the function of cilia signal transduction. Various signaling pathways such as Hedgehog, Wnt, PDGF, and mTOR have been reported to be related to primary cilia [45, 46]. First, we detected the expressions of GLI family members in the Hedgehog signaling pathway. The expressions of GLI1, 2, 3 increased remarkably in the PKD kidneys, and 1-Indanone down-regulated the over-activated molecules in Hedgehog signaling (Fig. 9a–c). Wnt/β-catenin is another signaling pathway closely related to primary cilia [47, 48]. Our results showed that the expressions of active (non-phosphorylated) β-catenin, total β-catenin and its downstream molecules c-myc and cyclin D1 were up-regulated in PKD kidneys. 1-Indanone notably reversed the increased expression of active β-catenin, total β-catenin and cyclin D1. The phosphorylation level of gsk-3β increased markedly in PKD, and was also retarded by 1-Indanone. It was confirmed that Wnt signal was activated in PKD and returned to normal level under the treatment of 1-Indanone. These data indicated that 1-Indanone suppressed the up-regulation of ciliary coordinated signaling pathways in PKD (Fig. 9d).

DISCUSSION

The goals of this study were to find active compounds with efficacy to retard cyst development in ADPKD from the natural compounds with anti-tumor activity and to determine the pharmacological mechanisms. We used distinct in vitro and in vivo experimental models of PKD to obtain proof of natural products as PKD therapeutics. By screening candidate compounds

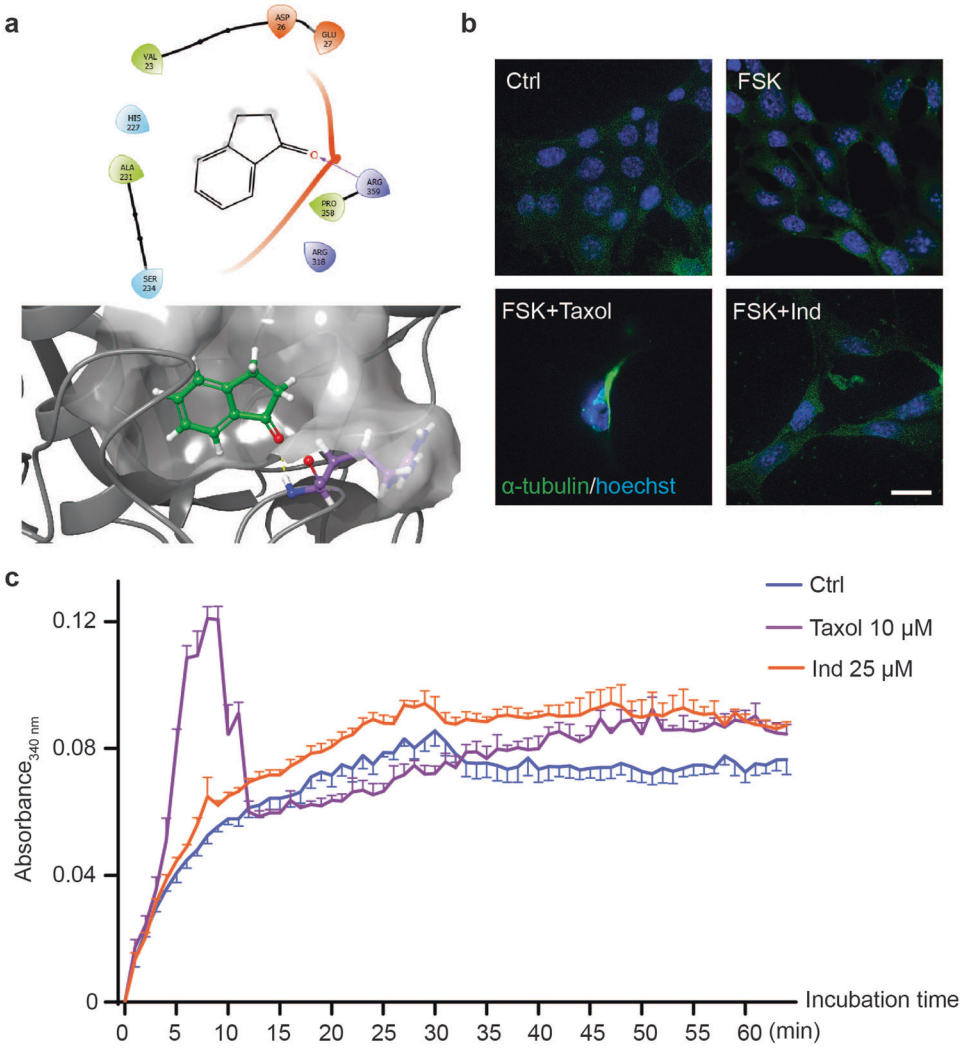

Fig. 7 1-Indanone modulates the structure of primary cilia by stabilizing tubulin. a Virtual docking results showing 1-Indanone formed a hydrogen bond with arginine at 359 in the paclitaxel binding site of tubulin (PDB ID: 6EW0). **b** Representative immunofluorescence images of α-tubulin in mIMCD cells (Ctrl) and FSK-treated mIMCD cells (FSK) incubated with 10 μM of paclitaxel (FSK+Taxol) or 25 μM of 1-Indanone (FSK+Ind). Bar = 20 μm. **c** The absorbance curves of tubulin treated with 1-Indanone (25 μM) incubated under 37 °C for 65 min at 340 nm.

that strongly inhibited cyst formation and growth in vivo and in vitro, without cytotoxicity, compound 1-Indanone was found to have the best efficacy in inhibiting cyst development.

Previous studies have found that some natural products with anti-tumor activity, such as *Curcumin, Ganoderma triterpenes* and *Cardamonin* [49–51], slowed down the development of renal cyst in ADPKD. These data suggest that the natural compounds with anti-tumor activity might slow down the development of renal cyst in ADPKD. In this study, based on the inhibitory effect on the signaling pathways modulating cellular abnormal proliferation both in tumor cells and renal cystic cells, we found an active compound 1-Indanone from the natural product library. 1-Indanone is isolated from marine cyanobacteria *Lyngbya majuscule* [52, 53]. Indanone analogs possess a variety of biological activities, which include anti-tumor, anti-Alzheimer's disease, anti-inflammation, anti-bacteria and anti-malaria. Previous studies reported that 1-Indanone inhibited the growth of various tumor cell lines by suppressing cell proliferation, arresting cell cycle in G_2/M phases [54]. In this study, it was found that 1-Indanone had a considerable inhibitory activity on the renal cyst development. In both in vitro MDCK cyst model and ex vitro embryonic kidney model, 1-Indanone reversibly inhibited the formation and growth of cysts in a dose-dependent manner. The experiments with *Pkd1* knockout mice confirmed that 1-Indanone markedly retarded the growth of renal cysts in vivo. Notably, our study found that 1-Indanone normalized the abnormal elongated primary cilia of cystic epithelial cells.

It is well established that primary cilium has a critical role in maintaining the normal function of the kidney. The primary cilium functions as a mechano-sensor in renal tubular epithelial cells to convert mechanical sensation into intracellular chemical signals [55]. Abnormalities of primary cilia of renal epithelial cells have been observed in various kidney diseases, such as acute tubular necrosis and unilateral nephrectomy [56–58]. Ciliopathies, such as Bardet-Biedl (BBS), Joubert (JBTS), Meckel-Gruber (MKS), are often accompanied by cystic kidney and defects of cilia biogenesis and ciliary assembly genes will lead to ADPKD, suggesting that defect in primary cilium is an important trigger of renal cyst development [22, 59–61].

However, the relationship between primary cilia length and renal cysts formation in PKD remains elusive. In PKD, cyst formation is driven by cAMP-mediated hyperproliferation of cystic

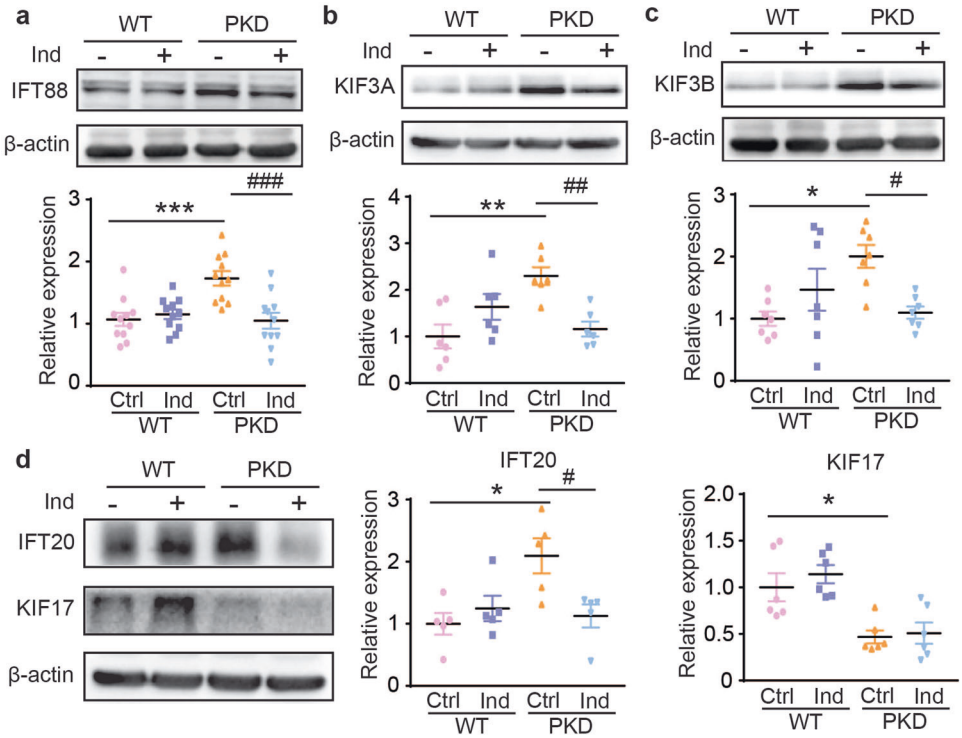

Fig. 8 1-Indanone down-regulates anterograde transport of primary cilia. a Representative Western blots and relative protein expression of IFT88 in the kidneys of wild-type (WT) and PKD mice without (Ctrl) or with 1-Indanone (Ind) treatment. $n = 11$. **b** Representative Western blots and relative protein expression of KIF3A. **c** Representative Western blots and relative and protein expression of KIF3B. $n \geq 6$. **d** Representative Western blots and relative protein expression of IFT20 and KIF17. $n = 5–6$. All data are presented by mean values ± SEM. $^{*}P < 0.05$, $^{**}P < 0.01$, $^{***}P < 0.001$ vs. Ctrl group in WT mice, $^{\#}P < 0.05$, $^{\#\#}P < 0.01$, $^{\#\#\#}P < 0.001$ vs. Ctrl group in PKD mice.

epithelial cells [34]. It is reported that the activation of cAMP or PKA will conspicuously prolong primary cilia [62]. And studies have shown that down-regulating TSC1/TSC2, negative regulators of mTORC1 promoted the elongation of cilia [36] and administration with mTORC1 inhibitor rapamycin reversed the increase of primary cilia length [63]. Therefore, it indicated in our study that the over-activated mTOR signaling in ADPKD renal tubular epithelial cells may contribute to the abnormalities of primary cilia length. Conversely, defects of primary cilia structure will promote cyst expansion in ADPKD, suggesting there is a regulatory loop between primary cilia and cellular proliferation. In this study, 1-Indanone inhibited the excessive elongation of primary cilia in cystic epithelial cells. Simultaneously, 1-Indanone suppressed the activation of the cAMP/PKA, and down-regulated mTOR signaling pathways and retarded the resulting cellular hyperproliferation. Thus, 1-Indanone broke the regulatory loop between the hyperproliferation and primary cilia elongation in renal cystic epithelial cells.

The assembly and elongation of cilia depend on the anterograde or retrograde transport of component proteins. Previous studies showed that inhibiting efficiently the expression of primary cilia-related proteins KIF3A, IFT88, IFT20 in *Pkd1* or *Pkd2* knockout mice suppressed renal cyst progression [24, 64], suggesting modulating the transport process of the primary cilia component proteins may be a therapeutic approach for ADPKD. Our study found that the expressions of IFT88, IFT20, KIF3A and KIF3B were notably up-regulated in PKD mouse kidney, which were down-regulated by 1-Indanone. The experimental results indicate that 1-Indanone reduced the abnormal cilium length by affecting primary cilium assembly. The cell cycle is another factor that closely affects the biogenesis and assembly of primary cilia. The primary cilia are assembled in the G_0/G_1 phase and reabsorbed into the cell entering S phase [65]. Recently, several studies have illustrated that the cell cycle-dependent kinases that modulate the G_1-S cell cycle transition promote the cyst formation in ADPKD [66–68]. In this study, we verified that with FSK stimulation, the cells in G_0/G_1 phases were increased remarkably compared with ctrl group, which indicated except for excessively increase in cilia length, ciliogenesis in cystic epithelial cells was also elevated. 1-Indanone inhibited the increase in G_0/G_1 phase cell number induced by FSK treatment, illustrating that 1-Indanone may inhibit ciliogenesis in cystic epithelial cells by cell cycle arresting.

The primary cilium is a microtubule-based organelle. Cilium assembly depends on importing tubulin to cilium axoneme and tubulin at cilium tip. It has been reported the microtubule stabilizer strikingly reduced the length of primary cilia [69], and retarded renal cysts expansion in PKD [70]. Our previous target prediction for 1-Indanone from "Similarity Ensemble Approach server database" indicated that 1-Indanone might bind to the heavy chain of α-tubulin. Our docking results showed 1-Indanone formed a hydrogen bond with arginine at 359 in the paclitaxel binding site of tubulin, which suggests that 1-Indanone might promote tubulin polymerization. In addition, we found that the expression of KIF17, another component of kinesin, is reduced in ADPKD. KIF17 has been reported to stabilize tubulin. Knocking out KIF17 in vitro leads to the formation of cysts [71]. All these data suggest that 1-Indanone inhibited the extension of primary cilia by down-regulating the anterograde transport of soluble tubulin along the cilia axoneme.

The primary cilium is considered as a hub of signaling transduction. A variety of oncogenic signaling coordinated with primary cilia, such as hedgehog and Wnt/β-catenin signaling pathways [72], both of which facilitate cyst development [73, 74].

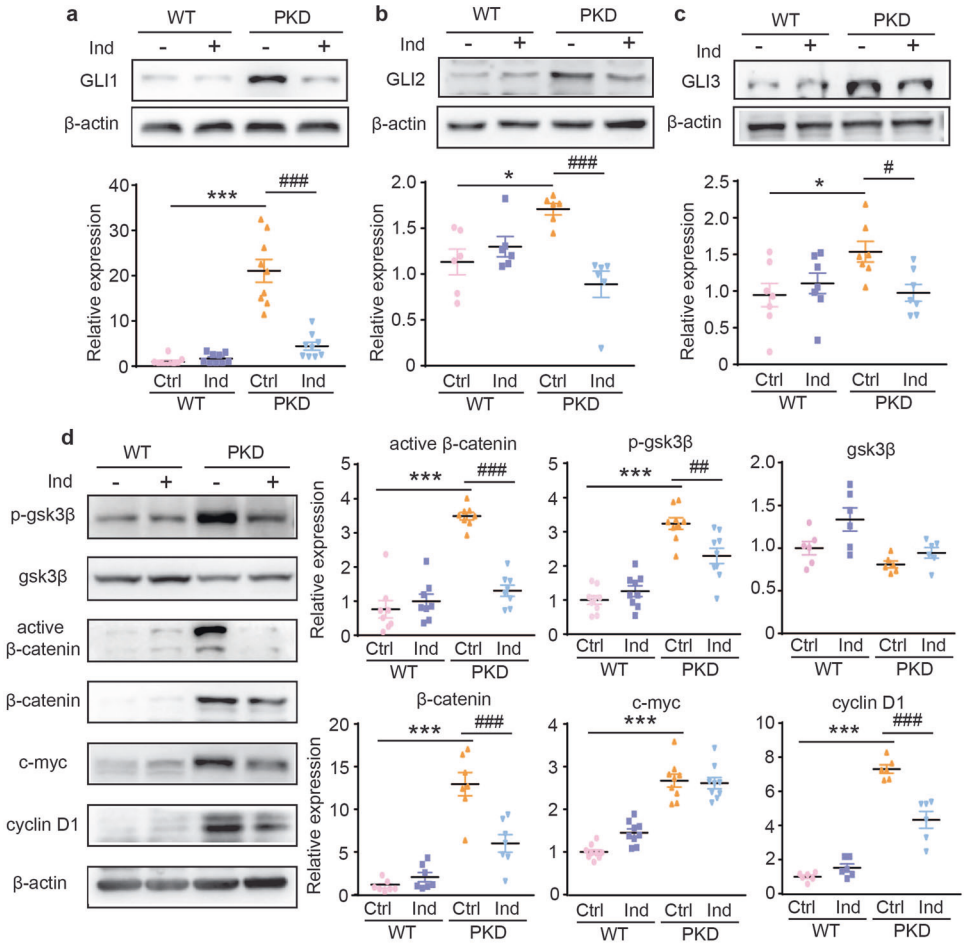

Fig. 9 1-Indanone down-regulates signaling pathways coordinated with primary cilia. a Representative Western blots and relative protein expression of GLI1 in wild-type (WT) and PKD kidneys treated without (Ctrl) or with 1-Indanone (Ind). $n \geq 6$. **b** Representative Western blots and relative protein expression of GLI2. $n \geq 6$. **c** Representative Western blots and relative protein expression of GLI3. $n \geq 6$. **d** Representative Western blots and relative protein expression of signature proteins in canonical Wnt signaling. $n \geq 6$. Data are presented by mean values ± SEM. $^{*}P < 0.05$, $^{***}P < 0.001$ vs. Ctrl group in WT mice, $^{\#}P < 0.05$, $^{\#\#}P < 0.01$, $^{\#\#\#}P < 0.001$ vs. Ctrl group in PKD mice.

It has been reported that the hedgehog signaling transduction relies on primary cilia [75, 76]. In this study, we found three GLI family members were up-regulated impressively in the kidneys of PKD mice, which were rescued by 1-Indanone. Besides, it is well elaborated that primary cilium played an important role in Wnt signaling transduction, and defects in cilia lead to over-activation of Wnt signaling [77, 78]. In our study, it was determined that 1-Indanone suppressed the activation of β-catenin and the increase of its downstream effector cyclin-D1 in PKD mice, which suggested 1-Indanone might influence cyst initiation regulated by β-catenin.

However, this study still has many limitations. First, whether there is a direct regulatory relationship between cytoskeletal dynamics and signaling pathways co-transduced by primary cilia remains to be investigated. In addition, the velocity of primary ciliary transport is also an important indicator for regulating ciliary biogenesis and assembly. However, due to limited experimental conditions, we did not detect it. ADPKD is a slowly progressive disease. The *Pkd1* knockout mice used in this study is a rapidly progressive model and can not accurately simulate the process of human ADPKD. We intend to examine the effect of 1-Indanone on primary cilia length as the cyst progresses using the slowly progressive ADPKD model in the future. Besides, it is also planned to examine the specific expression of hedgehog signaling and Wnt signaling effector molecules in cilia, but precise measurements may be difficult due to the limitations of current technology. Moreover, we may examine the pharmacokinetic characteristics of 1-Indanone by oral administration and optimize its chemical structure if necessary.

In conclusion, in this study we found the potential of 1-Indanone suppressing renal cyst development through in vitro and in vivo ADPKD models. 1-Indanone inhibited the abnormal elongation of primary cilia by stabilizing tubulin and decreasing anterograde transporting soluble tubulin to cilia axoneme, and suppressed the over-activation of ciliary coordinated hedgehog and Wnt signaling pathways. Therefore, 1-Indanone inhibited the ciliary defects in signal transduction and fluid sensation caused by alterations in the primary cilia structure. Thereby, 1-Indanone down-regulated the over-activation of cAMP/PKA and downstream MAPK and mTOR signaling pathways and regulated excessive proliferation in cystic epithelial cells. As a result, 1-Indanone broke the regulation loop between excessive cell proliferation and alteration in primary cilia structure. Eventually, 1-Indanone retarded renal cysts growth and delayed ADPKD progression (Fig. 10). Our data indicate that normalizing the length of primary cilia in cystic epithelial cells is a promising therapeutic strategy for ADPKD and 1-Indanone is a potential therapeutic candidate for ADPKD treatment.

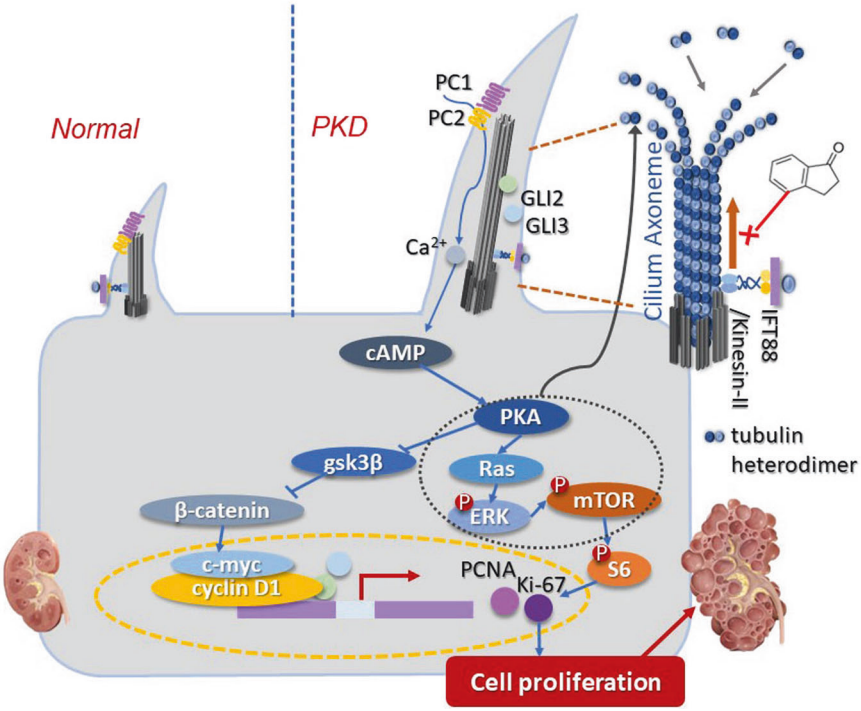

Fig. 10 The diagram of mechanism in which 1-Indanone delays cyst development in ADPKD. 1-Indanone inhibits the abnormal elongation of cystic epithelial cilia via blocking soluble tubulin transport to cilium axoneme, which down-regulates Wnt/β-catenin, hedgehog, Ras/MAPK and mTOR signaling pathways, eventually ameliorates the epithelial cell proliferation of renal cysts in ADPKD.

ACKNOWLEDGEMENTS

We thank Dr. Peter Igarashi (University of Minnesota) and Dr. Stefan Somlo (Yale School of Medicine) for providing us with the *Ksp*-Cre and *Pkd1*$^{flox/flox}$ mice. This work was supported by the National Natural Science Foundation of China grants (81974083, 81873597 and 81800388).

AUTHOR CONTRIBUTIONS

BXY and XWL designed the experiments. XWL performed the research and analyzed the data. XWL, HZ, JZH, ZWQ, SYW, SZ, YPA, AM, ML, YZQ, NNL, CQR and BXY interpreted the results. XWL and BXY drafted and edited the manuscript. JHR and MNW provided support for electron microscopy imaging techniques. All authors commented on and approved the final manuscript.

ADDITIONAL INFORMATION

Supplementary information The online version contains supplementary material available at https://doi.org/10.1038/s41401-022-00937-z.

Competing interests: The authors declare no competing interests.

REFERENCES

1. Cornec-Le Gall E, Alam A, Perrone RD. Autosomal dominant polycystic kidney disease. Lancet. 2019;393:919–35.
2. Bergmann C, Guay-Woodford LM, Harris PC, Horie S, Peters DJM, Torres VE. Polycystic kidney disease. Nat Rev Dis Prim. 2018;4:50.
3. Dong K, Zhang C, Tian X, Coman D, Hyder F, Ma M, et al. Renal plasticity revealed through reversal of polycystic kidney disease in mice. Nat Genet. 2021;53:1649–63.
4. Torres VE, Harris PC, Pirson Y. Autosomal dominant polycystic kidney disease. Lancet. 2007;369:1287–301.
5. Torres VE, Harris PC. Progress in the understanding of polycystic kidney disease. Nat Rev Nephrol. 2019;15:70–2.
6. Yoder BK, Hou X, Guay-Woodford LM. The polycystic kidney disease proteins, polycystin-1, polycystin-2, polaris, and cystin, are co-localized in renal cilia. J Am Soc Nephrol. 2002;13:2508–16.
7. Nauli SM, Alenghat FJ, Luo Y, Williams E, Vassilev P, Li X, et al. Polycystins 1 and 2 mediate mechano-sensation in the primary cilium of kidney cells. Nat Genet. 2003;33:129–37.
8. Fliegauf M, Benzing T, Omran H. When cilia go bad: cilia defects and ciliopathies. Nat Rev Mol Cell Biol. 2007;8:880–93.
9. Bergmann C, Guay-Woodford LM, Harris PC, Horie S, Peters DJM, Torres VE. Polycystic kidney disease. Nat Rev Dis Prim. 2018;4:50.
10. Cloutier M, Manceur AM, Guerin A, Aigbogun MS, Oberdhan D, Gauthier M. The societal economic burden of autosomal dominant polycystic kidney disease in the United States. BMC Health Serv Res. 2020;20:126.
11. Chapman AB, Devuyst O, Eckardt KU, Gansevoort RT, Harris T, Horie S, et al. Autosomal-dominant polycystic kidney disease (ADPKD): executive summary from a kidney disease: Improving global outcomes (KDIGO) controversies conference. Kidney Int. 2015;88:17–27.
12. Torres VE, Chapman AB, Devuyst O, Gansevoort RT, Perrone RD, Koch G, et al. REPRISE Trial Investigators. Tolvaptan in later-stage autosomal dominant polycystic kidney disease. N Engl J Med. 2017;377:1930–42.
13. Torres VE, Chapman AB, Devuyst O, Gansevoort RT, Grantham JJ, Higashihara E, et al. TEMPO 3:4 Trial Investigators. Tolvaptan in patients with autosomal dominant polycystic kidney disease. N Engl J Med. 2012;367:2407–18.
14. Torres VE, Gansevoort RT, Perrone RD, Chapman AB, Ouyang J, Lee J, et al. Tolvaptan in ADPKD patients with very low kidney function. Kidney Int Rep. 2021;6:2171–8.
15. Gansevoort RT, Arici M, Benzing T, Birn H, Capasso G, Covic A, et al. Recommendations for the use of tolvaptan in autosomal dominant polycystic kidney disease: a position statement on behalf of the ERA-EDTA working groups on inherited kidney disorders and European renal best practice. Nephrol Dial Transpl. 2016;31:337–48.
16. Mustafa RA, Yu ASL. Burden of proof for Tolvaptan in ADPKD: did REPRISE provide the answer? Clin J Am Soc Nephrol. 2018;13:1107–9.
17. Perrone RD, Abebe KZ, Watnick TJ, Althouse AD, Hallows KR, Lalama CM, et al. Primary results of the randomized trial of metformin administration in polycystic kidney disease (TAME PKD). Kidney Int. 2021;100:684–96.
18. Arroyo J, Escobar-Zarate D, Wells HH, Constans MM, Thao K, Smith JM, et al. The genetic background significantly impacts the severity of kidney cystic disease in the *Pkd1*$^{RC/RC}$ mouse model of autosomal dominant polycystic kidney disease. Kidney Int. 2021;99:1392–407.
19. Wang J, Tripathy N, Chung EJ. Targeting and therapeutic peptide-based strategies for polycystic kidney disease. Adv Drug Deliv Rev. 2020;161-2:176–89.

20. Seeger-Nukpezah T, Geynisman DM, Nikonova AS, Benzing T, Golemis EA. The hallmarks of cancer: relevance to the pathogenesis of polycystic kidney disease. Nat Rev Nephrol. 2015;11:515–34.
21. Higgins M, Obaidi I, McMorrow T. Primary cilia and their role in cancer. Oncol Lett. 2019;17:3041–7.
22. Hildebrandt F, Benzing T, Katsanis N. Ciliopathies. N Engl J Med. 2011;364:1533–43.
23. Wang S, Dong Z. Primary cilia and kidney injury: current research status and future perspectives. Am J Physiol Ren Physiol. 2013;305:F1085–98.
24. Ma M, Tian X, Igarashi P, Somlo S. Loss of cilia suppresses cyst growth in genetic models of autosomal dominant polycystic kidney disease. Nat Genet. 2013;45:1004–12.
25. Lehman JM, Michaud EJ, Schoeb TR, Aydin-Son Y, Miller M, Yoder BK. The Oak Ridge Polycystic Kidney mouse: modeling ciliopathies of mice and men. Dev Dyn. 2008;237:1960–71.
26. Hopp K, Ward CJ, Hommerding CJ, Nasr SH, Tuan HF, Gainullin VG, et al. Functional polycystin-1 dosage governs autosomal dominant polycystic kidney disease severity. J Clin Invest. 2012;122:4257–73.
27. Smith LA, Bukanov NO, Husson H, Russo RJ, Barry TC, Taylor AL, et al. Development of polycystic kidney disease in juvenile cystic kidney mice: insights into pathogenesis, ciliary abnormalities, and common features with human disease. J Am Soc Nephrol. 2006;17:2821–31.
28. Liu X, Vien T, Duan J, Sheu SH, Decaen PG, Clapham DE. Polycystin-2 is an essential ion channel subunit in the primary cilium of the renal collecting duct epithelium. Elife. 2018;7:e33183.
29. Shao L, El-Jouni W, Kong F, Ramesh J, Kumar RS, Shen X, et al. Genetic reduction of cilium length by targeting intraflagellar transport 88 protein impedes kidney and liver cyst formation in mouse models of autosomal polycystic kidney disease. Kidney Int. 2020;98:1225–41.
30. Husson H, Moreno S, Smith LA, Smith MM, Russo RJ, Pitstick R, et al. Reduction of ciliary length through pharmacologic or genetic inhibition of CDK5 attenuates polycystic kidney disease in a model of nephronophthisis. Hum Mol Genet. 2016;25:2245–55.
31. Yang B, Sonawane ND, Zhao D, Somlo S, Verkman AS. Small-molecule CFTR inhibitors slow cyst growth in polycystic kidney disease. J Am Soc Nephrol. 2008;19:1300–10.
32. Shelanski ML, Gaskin F, Cantor CR. Microtubule assembly in the absence of added nucleotides. Proc Natl Acad Sci USA. 1973;70:765–8.
33. Silva LM, Wang W, Allard BA, Pottorf TS, Jacobs DT, Tran PV. Analysis of primary cilia in renal tissue and cells. Methods Cell Biol. 2019;153:205–29.
34. Calvet JP. The role of calcium and cyclic AMP in PKD. In: Li X, editor. Polycystic kidney disease. Chapter 8. Brisbane (AU): Codon Publications; 2015.
35. Yoder BK. Role of primary cilia in the pathogenesis of polycystic kidney disease. J Am Soc Nephrol. 2007;18:1381–8.
36. Yuan S, Li J, Diener DR, Choma MA, Rosenbaum JL, Sun Z. Target-of-rapamycin complex 1 (Torc1) signaling modulates cilia size and function through protein synthesis regulation. Proc Natl Acad Sci USA. 2012;109:2021–6.
37. Abdul-Majeed S, Moloney BC, Nauli SM. Mechanisms regulating cilia growth and cilia function in endothelial cells. Cell Mol Life Sci. 2012;69:165–73.
38. Sharma N, Bryant J, Wloga D, Donaldson R, Davis RC, Jerka-Dziadosz M, et al. Katanin regulates dynamics of microtubules and biogenesis of motile cilia. J Cell Biol. 2007;178:1065–79.
39. Lee K, Battini L, Gusella GL. Cilium, centrosome and cell cycle regulation in polycystic kidney disease. Biochim Biophys Acta. 2011;1812:1263–71.
40. Ishikawa H, Marshall WF. Intraflagellar transport and ciliary dynamics. Cold Spring Harb Perspect Biol. 2017;9:a021998.
41. Follit JA, Tuft RA, Fogarty KE, Pazour GJ. The intraflagellar transport protein IFT20 is associated with the Golgi complex and is required for cilia assembly. Mol Biol Cell. 2006;17:3781–92.
42. Lu H, Toh MT, Narasimhan V, Thamilselvam SK, Choksi SP, Roy S. A function for the Joubert syndrome protein Arl13b in ciliary membrane extension and ciliary length regulation. Dev Biol. 2015;397:225–36.
43. Larkins CE, Aviles GD, East MP, Kahn RA, Caspary T. Arl13b regulates ciliogenesis and the dynamic localization of Shh signaling proteins. Mol Biol Cell. 2011;22:4694–703.
44. Berbari NF, Sharma N, Malarkey EB, Pieczynski JN, Boddu R, Gaertig J, et al. Microtubule modifications and stability are altered by cilia perturbation and in cystic kidney disease. Cytoskeleton. 2013;70:24–31.
45. Wheway G, Nazlamova L, Hancock JT. Signaling through the primary cilium. Front Cell Dev Biol. 2018;6:8.
46. Tran PV, Talbott GC, Turbe-Doan A, Jacobs DT, Schonfeld MP, Silva LM, et al. Downregulating hedgehog signaling reduces renal cystogenic potential of mouse models. J Am Soc Nephrol. 2014;25:2201–12.
47. Kyun ML, Kim SO, Lee HG, Hwang JA, Hwang J, Soung NK, et al. Wnt3a stimulation promotes primary ciliogenesis through β-catenin phosphorylation-induced reorganization of centriolar satellites. Cell Rep. 2020;30:1447–62.e5.
48. Lee EJ, Seo E, Kim JW, Nam SA, Lee JY, Jun J, et al. TAZ/Wnt-β-catenin/c-MYC axis regulates cystogenesis in polycystic kidney disease. Proc Natl Acad Sci USA. 2020;117:29001–12.
49. Gao J, Zhou H, Lei T, Zhou L, Li W, Li X, et al. Curcumin inhibits renal cyst formation and enlargement in vitro by regulating intracellular signaling pathways. Eur J Pharmacol. 2011;654:92–9.
50. Su L, Liu L, Jia Y, Lei L, Liu J, Zhu S, et al. Ganoderma triterpenes retard renal cyst development by downregulating Ras/MAPK signaling and promoting cell differentiation. Kidney Int. 2017;92:1404–18.
51. He J, Zhou H, Meng J, Zhang S, Li X, Wang S, et al. Cardamonin retards progression of autosomal dominant polycystic kidney disease via inhibiting renal cyst growth and interstitial fibrosis. Pharmacol Res. 2020;155:104751.
52. Luesch H, Yoshida WY, Moore RE, Paul VJ, Mooberry SL. Isolation, structure determination, and biological activity of Lyngbyabellin A from the marine cyanobacterium lyngbya majuscula. J Nat Prod. 2000;63:611–5.
53. Nagle DG, Zhou YD, Park PU, Paul VJ, Rajbhandari I, Duncan CJ, et al. A new Indanone from the marine cyanobacterium Lyngbya majuscula that inhibits hypoxia-induced activation of the VEGF promoter in Hep3B cells. J Nat Prod. 2000;63:1431–3.
54. Patil SA, Patil R, Patil SA. Recent developments in biological activities of Indanones. Eur J Med Chem. 2017;138:182–98.
55. Delling M, DeCaen PG, Doerner JF, Febvay S, Clapham DE. Primary cilia are specialized calcium signalling organelles. Nature. 2013;504:311–4.
56. Verghese E, Ricardo SD, Weidenfeld R, Zhuang J, Hill PA, Langham RG, et al. Renal primary cilia lengthen after acute tubular necrosis. J Am Soc Nephrol. 2009;20:2147–53.
57. Verghese E, Weidenfeld R, Bertram JF, Ricardo SD, Deane JA. Renal cilia display length alterations following tubular injury and are present early in epithelial repair. Nephrol Dial Transpl. 2008;23:834–41.
58. Han SJ, Jang HS, Kim JI, Lipschutz JH, Park KM. Unilateral nephrectomy elongates primary cilia in the remaining kidney via reactive oxygen species. Sci Rep. 2016;6:22281.
59. Duong Phu M, Bross S, Burkhalter MD, Philipp M. Limitations and opportunities in the pharmacotherapy of ciliopathies. Pharmacol Ther. 2021;225:107841.
60. Li Y, Tian X, Ma M, Jerman S, Kong S, Somlo S, et al. Deletion of ADP ribosylation factor-like GTPase 13B leads to kidney cysts. J Am Soc Nephrol. 2016;27:3628–38.
61. Lin F, Hiesberger T, Cordes K, Sinclair AM, Goldstein LS, Somlo S, et al. Kidney-specific inactivation of the KIF3A subunit of kinesin-II inhibits renal ciliogenesis and produces polycystic kidney disease. Proc Natl Acad Sci USA. 2003;100:5286–91.
62. Besschetnova TY, Kolpakova-Hart E, Guan Y, Zhou J, Olsen BR, Shah JV. Identification of signaling pathways regulating primary cilium length and flow-mediated adaptation. Curr Biol. 2010;20:182–7.
63. Rosengren T, Larsen LJ, Pedersen LB, Christensen ST, Møller LB. TSC1 and TSC2 regulate cilia length and canonical Hedgehog signaling via different mechanisms. Cell Mol Life Sci. 2018;75:2663–80.
64. Jonassen JA, San Agustin J, Follit JA, Pazour GJ. Deletion of IFT20 in the mouse kidney causes misorientation of the mitotic spindle and cystic kidney disease. J Cell Biol. 2008;183:377–84.
65. Plotnikova OV, Pugacheva EN, Golemis EA. Primary cilia and the cell cycle. Methods Cell Biol. 2009;94:137–60.
66. Zhang C, Balbo B, Ma M, Zhao J, Tian X, Kluger Y, et al. Cyclin-dependent kinase 1 activity is a driver of cyst growth in polycystic kidney disease. J Am Soc Nephrol. 2021;32:41–51.
67. Zhang JQJ, Burgess J, Stepanova D, Saravanabavan S, Wong ATY, Kaldis P, et al. Role of cyclin-dependent kinase 2 in the progression of mouse juvenile cystic kidney disease. Lab Invest. 2020;100:696–711.
68. Li LX, Zhou JX, Wang X, Zhang H, Harris PC, Calvet JP, et al. Cross-talk between CDK4/6 and SMYD2 regulates gene transcription, tubulin methylation, and ciliogenesis. Sci Adv. 2020;6:eabb3154.
69. Sharma N, Kosan ZA, Stallworth JE, Berbari NF, Yoder BK. Soluble levels of cytosolic tubulin regulate ciliary length control. Mol Biol Cell. 2011;22:806–16.
70. Woo DD, Miao SY, Pelayo JC, Woolf AS. Taxol inhibits progression of congenital polycystic kidney disease. Nature. 1994;368:750–3.
71. Jaulin F, Kreitzer G. KIF17 stabilizes microtubules and contributes to epithelial morphogenesis by acting at MT plus ends with EB1 and APC. J Cell Biol. 2010;190:443–60.
72. Ma M, Gallagher AR, Somlo S. Ciliary mechanisms of cyst formation in polycystic kidney disease. Cold Spring Harb Perspect Biol. 2017;9:a028209.
73. Li A, Xu Y, Fan S, Meng J, Shen X, Xiao Q, et al. Canonical Wnt inhibitors ameliorate cystogenesis in a mouse ortholog of human ADPKD. JCI Insight. 2018;3:e95874.
74. Silva LM, Jacobs DT, Allard BA, Fields TA, Sharma M, Wallace DP, et al. Inhibition of Hedgehog signaling suppresses proliferation and microcyst formation of human Autosomal Dominant Polycystic Kidney Disease cells. Sci Rep. 2018;8:4985.
75. Bangs F, Anderson KV. Primary cilia and mammalian Hedgehog signaling. Cold Spring Harb Perspect Biol. 2017;9:a028175.

76. Anvarian Z, Mykytyn K, Mukhopadhyay S, Pedersen LB, Christensen ST. Cellular signalling by primary cilia in development, organ function and disease. Nat Rev Nephrol. 2019;15:199–219.
77. Abdelhamed ZA, Wheway G, Szymanska K, Natarajan S, Toomes C, Inglehearn C, et al. Variable expressivity of ciliopathy neurological phenotypes that encompass Meckel-Gruber syndrome and Joubert syndrome is caused by complex de-regulated ciliogenesis, Shh and Wnt signalling defects. Hum Mol Genet. 2013;22:1358–72.
78. Wheway G, Abdelhamed Z, Natarajan S, Toomes C, Inglehearn C, Johnson CA. Aberrant Wnt signalling and cellular over-proliferation in a novel mouse model of Meckel-Gruber syndrome. Dev Biol. 2013;377:55–66.